

Influence of the branches width on the nonlinear output characteristics of InAlAs/InGaAs-based three-terminal junctions

I. Iñiguez-de-la-Torre,¹ T. González,¹ D. Pardo,¹ C. Gardès,² Y. Roelens,² S. Bollaert,² and J. Mateos^{1,a)}

¹*Departamento de Física Aplicada, Universidad de Salamanca, Plaza de la Merced s/n, 37008 Salamanca, Spain*

²*Département Hyperfréquences et Semiconducteurs, Institut d'Electronique de Microélectronique et de Nanotechnologie (IEMN), Avenue Poincaré BP60069, 59652, Villeneuve d'Ascq CEDEX, France*

(Received 27 November 2008; accepted 26 March 2009; published online 6 May 2009)

In this work, the influence of the geometry of the different branches on the output characteristics of InAlAs/InGaAs three-branch junctions is analyzed. At room temperature experimental measurements show that when increasing the width of the horizontal branches, the nonlinear behavior persists, even if less pronounced. This implies a reduction in the (typically high) impedance of these nanodevices, which is quite interesting in order to minimize the influence of parasitic capacitances on their cutoff frequency and to decrease the reflected power due to the mismatch with the 50 Ω standard equipment. The width of the vertical branch is also a relevant parameter, nonlinear effects being more important for narrow branches. In both cases surface charges at the etched boundaries of the branches play a key role. Monte Carlo simulations (performed with a self-consistent surface charge model recently proposed by the authors) are used to explain the physical origin of the observed behavior and to improve the device performance. We focus on the enhancement of their efficiency as a way to develop their promising functionalities in various analog and digital circuits. © 2009 American Institute of Physics.

[DOI: [10.1063/1.3124363](https://doi.org/10.1063/1.3124363)]

I. INTRODUCTION

In the past years a number of experiments have demonstrated nonlinear effects in ballistic nanostructures that are quite robust at room temperature.¹⁻³ One of them is the T-shaped three-terminal junction (TBJ), which has attracted considerable attention as a possible building block of analog and digital integrated circuits,⁴ with particular potentiality for operation at extremely high frequencies.⁵ This nanodevice exhibits an interesting nonlinear effect related to the presence of ballistic transport: a parabolic down bending of the output voltage at the open-circuited central branch when biasing horizontal branches in push-pull fashion.⁶⁻⁸ This feature is highly attractive for applications like terahertz detection or frequency doubling, for which a strongly parabolic response is desirable. To this end, the size (length and width) of the different branches of TBJs should be optimized, since it plays an important role in their nonlinear properties. While several experimental and theoretical studies have been performed to analyze the influence of the length of the horizontal branches^{6,9} and the width of the vertical branch,¹⁰ less attention has been paid to the width of the horizontal branches W_H , even if this parameter may be essential to improve the high-frequency performance of TBJs. Indeed, one of the main problems of these nanodevices is their very high input impedance (typically of the order of kilohms), which leads to a strong mismatch with 50 Ω standard equipment, with the consequent loss in efficiency because of power reflection. Moreover, the intrinsically very high cutoff frequen-

cies of the devices are quite degraded by such high impedances, which lead to long extrinsic time constants when coupled to the parasitic capacitances of the contacts (which cannot be reduced below the femtofarad range). By increasing W_H , the input impedance could be significantly reduced; however, the efficiency of nonlinear effects decrease, so that its value should be carefully chosen.

The objective of this work is to analyze, both experimentally and theoretically, which is the influence of the width of the horizontal branch on the nonlinear effects observed in InAlAs/InGaAs TBJs. Additionally, the role played by the width of the vertical branch W_V will also be studied. To this end, TBJs with different sizes of both horizontal and vertical branches have been fabricated and characterized. We have found that, even if the efficiency is reduced, the down bending parabolic behavior of the output voltage is still observed in devices with values of W_H higher than 1 μm . To explain such a behavior, the consideration of surface charges at the etched boundaries of the different branches is essential, and theoretical models accounting for them must be used.

One possibility for the description of these ballistic devices is a coherent transport picture;¹¹ however, such an approach has a limited application and is not able to explain some of the observed dependences.⁶ In particular, the influence of surface charges is not considered. As an alternative, in this work we will use a microscopic semiclassical Monte Carlo (MC) tool for the modeling the electron transport properties in nanodevices,⁷⁻⁹ which includes a recently developed self-consistent technique to account for the influence of surface charges.¹⁰

The paper is organized as follows. In Sec. II, the details

^{a)}Electronic mail: javierm@usal.es.

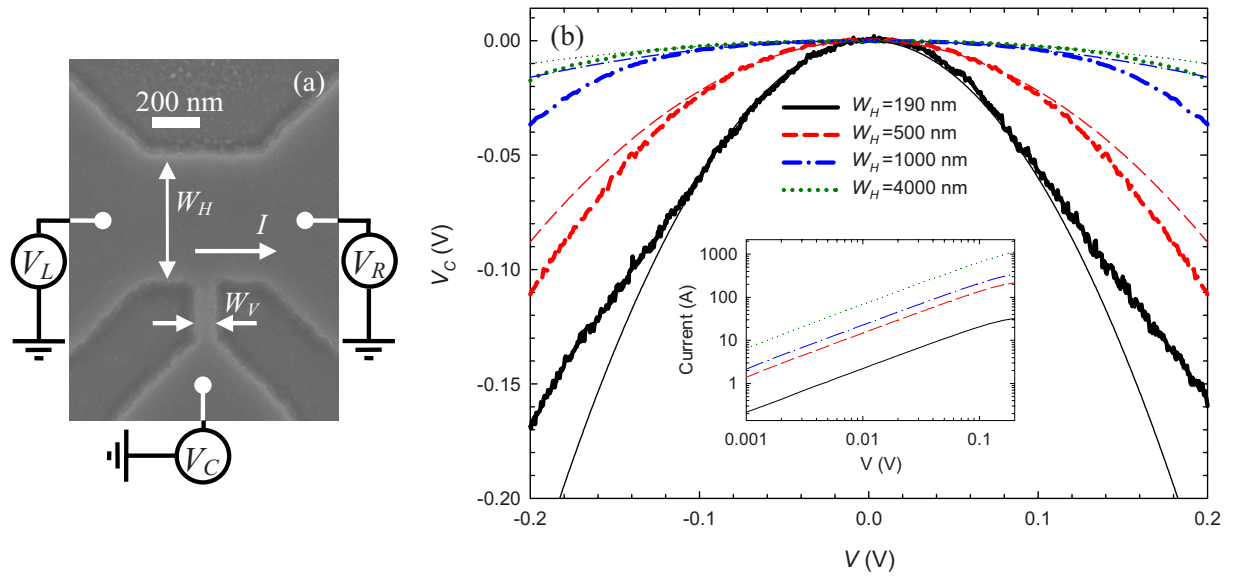


FIG. 1. (Color online) (a) SEM image of one of the fabricated TBJs. (b) Values of the bottom potential V_C and current I (inset) measured in TBJ junctions with $W_H=190, 500, 1000,$ and 4000 nm as a function of the push-pull bias V . The width of the vertical branch W_V is approximately the same, 70 nm. Hair lines show parabolic fittings.

of the technological fabrication process and the physical model used in MC simulations are described. In Sec. III, the results obtained from the static characterization of junctions with different sizes are reported. The theoretical interpretation of the results in terms of the information provided by MC simulations is presented in Sec. IV. Finally, Sec. V summarizes the main conclusions.

II. DEVICE STRUCTURE AND PHYSICAL MODEL FOR THE SIMULATION

TBJs have been fabricated on an $\text{In}_{0.52}\text{Al}_{0.48}\text{As}/\text{In}_{0.75}\text{Ga}_{0.25}\text{As}$ heterostructure grown by molecular beam epitaxy,⁵ with particularly high mobility and n_s (around $14\,000\text{ cm}^2/\text{V s}$ and $2.5 \times 10^{12}\text{ cm}^{-2}$, respectively, at room temperature) due to the large In content in the channel material. For the fabrication of the devices, a metallic pattern defined with a Leica EBPG5000+ is transferred to a silicon nitride layer used as a mask, then the epilayer is etched by reactive ion etching (RIE) with $\text{CH}_4/\text{H}_2/\text{Ar}$ plasma in order to isolate and define the TBJs. RIE has been preferred to wet etching because of the lower shape roughness, the better control of undercut, and the absence of transport degradation by plasma.⁵ A Ni-Ge-Au-Ni-Au metal sequence is deposited by evaporation and annealed at $300\text{ }^\circ\text{C}$ with a N_2H_2 gas to form Ohmic contacts. Finally, Ti-Au bonding pads are evaporated. Structures with width of the horizontal branch W_H ranging between 170 and 4000 nm and of the vertical branch W_V between 69 and 100 nm were fabricated. Figure 1(a) shows a picture in which the dimensions of one of the realized devices have been measured by scanning electron microscope (SEM).

TBJs are operated by applying an input voltage in a push-pull fashion, i.e., with a voltage $V_R=V$ applied to the right contact and a voltage $V_L=-V$ to the left one. The voltage at the bottom of the central branch V_C is measured as output with a high impedance voltmeter. For low input volt-

ages the output shows a bell-shaped dependence on V , remaining always negative, $V_C=-\alpha V^2/2$, where α is the curvature.^{2,6,10} This is an important parameter, since in order to obtain high sensitivity of signal detection a large α is required. For high applied voltages, negative values exhibiting a linear dependence on V , with a slope close to unity, have been predicted and measured.^{6,9,12}

As a tool to interpret the measured results we will make use of an ensemble MC simulator self-consistently coupled with a Poisson solver, already used to satisfactorily explain the behavior of TBJs and other nanodevices.⁷⁻⁹ Two-dimensional (2D) simulations are performed only in the InGaAs channel, and the influence of the fixed charges present in other layers is accounted for by means of a “background doping.” Details about the model can be found in Refs. 7 and 8. The depletion of the channel originated by the action of the lateral surface charge at the semiconductor-air interfaces may have a dramatic influence in the final response of the device. A simple way to include the influence of this surface charge in MC simulations is to consider a model in which a negative surface charge density σ is fixed to the experimentally extracted equilibrium value¹³ and kept constant independently of the topology of the structure, position along the interface, bias, and time. This surface charge is included as a Neumann boundary condition for the Poisson equation: $\varepsilon_2 E_2^n - \varepsilon_1 E_1^n = \sigma$, with ε_i as the permittivity and E_i^n as the normal electric field in the i th material. Nevertheless, for narrow channels the applicability of this model becomes doubtful when the width becomes lower than the depletion originated by this fixed surface charge.

To implement surface charge more precisely in MC simulations, at a detailed microscopic level, many difficulties arise. The properties of the traps as density, cross section, and energy distribution must be known, which is not our case. In addition, the capture and emission mean times of surface states (with values typically in the microsecond

range) are much higher than scattering times, thus preventing their detailed treatment in a microscopic MC scheme, since a huge computing time would be necessary to take into account the correct dynamics of these states. For these reasons, we have recently developed a model, based on the depletion induced by traps and not on their statistics, in which the local value of the surface charge at the interfaces is locally updated in a self-consistently way with the carrier dynamics near the boundaries during the simulation.¹⁰ In this way, the value of the surface charge changes with the position at the interface and, what is important, also with the bias. The philosophy of the model is as follows. Every given number of iterations, the average carrier concentration at every mesh adjacent to the interface is evaluated and compared to certain threshold values relative to the background doping. Upon the result of such a comparison, the surface charge can increase, decrease, or remain constant. In fact, the model tries to adapt electron concentration next to the interface to the range delimited by the defined thresholds. In this way, the surface charge evolves (increasing or decreasing in a given amount) until a stationary profile, adapted to the geometry of the device and the corresponding bias configuration, is reached. This model is not able to reproduce the statistics of occupation of surface states, but it does describe correctly the global effect of surface charge. A more detailed description can be found in Ref. 10.

III. EXPERIMENTAL RESULTS

A. Influence of the horizontal branch

Electrical measurements of the fabricated devices were performed at room temperature, at which the mean free path of electrons ℓ is about 150–200 nm in InGaAs. TBJs where horizontal branches are shorter or of the order of ℓ exhibit a parabolic down bending of the output voltage V_C in the low bias region.^{2,6} In our case, the length of the horizontal branches in the fabricated TBJs is always about 250 nm (570–600 nm from left to right contact by adding the width of the vertical branch), short enough to have quasiballistic transport and thus to expect a negative parabolic output voltage. In order to analyze the influence of the transversal size, TBJs have been fabricated with four different widths W_H of the horizontal branch (190, 500, 1000, and 4000 nm) and approximately the same width of the vertical branch, about 70 nm.

Figure 1(b) shows the V_C - V curves measured in the four TBJs, together with their parabolic fittings. The range of the applied potential is restricted to the low-bias region ($V < 0.2$ V), in which the ballistic/diffusive character of transport inside TBJs can be discriminated by the V_C - V behavior.^{6,9} At higher bias a linear dependence of V_C on V is typically found independently of the transport regime, which can be explained in terms of Γ - L intervalley transfer of electrons.⁹ As observed in the figure, the four structures exhibit a parabolic behavior, the curvature being higher as the width is decreased. From this result one may conclude that a narrow junction is in principle better for applications because of the higher efficiency. The curvature α obtained from the parabolic fittings is plotted in Fig. 2 as a function of W_H . It is

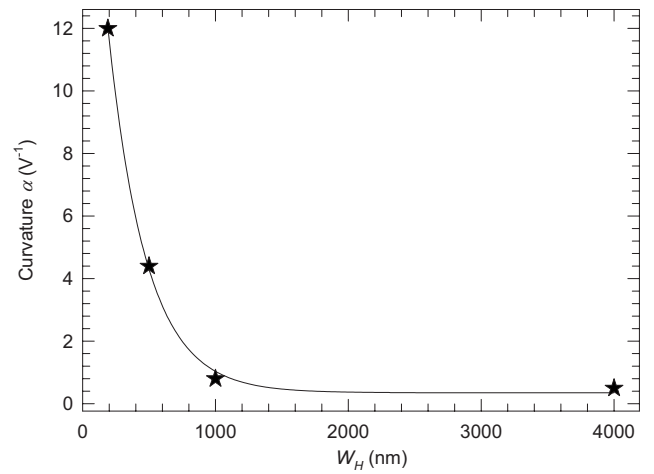


FIG. 2. Curvature factor α as a function of the width of the horizontal branch W_H . The continuous line shows the fitting according to Eq. (1).

remarkable that still when $W_H = 4.0$ μm the parabolic behavior is observed, even if with lower efficiency. This is expected, since the negative values of the potential are related to the presence of longitudinal (and not transversal) ballistic or quasiballistic transport, like our case. However, since the length of all the TBJs is identical, the origin of the down bending of V_C must be related not only to ballistic transport. As we will show later, these results can be interpreted in terms of a new factor: the strength of surface charge effects.

According to these two contributions to the parabolicity of the V_C - V response, the dependence of α on W_H has been fitted to a dependence of the type

$$\alpha(W_H) = \alpha_0 + K \exp(-W_H/W_0), \quad (1)$$

with α_0 , K , and W_0 being fitting parameters, taking values of 0.35 V^{-1} , 22.7 V^{-1} , and 285 nm, respectively. The contribution of longitudinal ballistic transport is represented by α_0 , and surface charge effects, which sharply decay when increasing W_H , by the exponential term with characteristic width W_0 .

The current flowing through the horizontal branches I is shown in the inset of Fig. 1(b) in log-log scale. As expected, it is higher for wider junctions and exhibits a linear dependence on V , with a tendency to saturation for the highest applied voltages (more significant the narrower the structure is). We also have measured the resistance associated to the horizontal branch R_H . The obtained values are 4.5, 1.4, 0.9, and 0.3 $k\Omega$ for $W_H = 190, 500, 1000,$ and 4000 nm, respectively. The reduction in the resistance with the increase in W_H while keeping the parabolic response may contribute to solve the problems related to the high impedance of TBJs in applications. Therefore, the value of W_H must be chosen as a trade-off between the required values of α and R_H for each specific application.

B. Influence of the vertical branch

In the previous results, the width of the vertical branch W_V is approximately 70 nm in the four junctions. In principle, one could think that the curvature of the parabolic V_C - V curve is independent of W_V , that is, the vertical branch

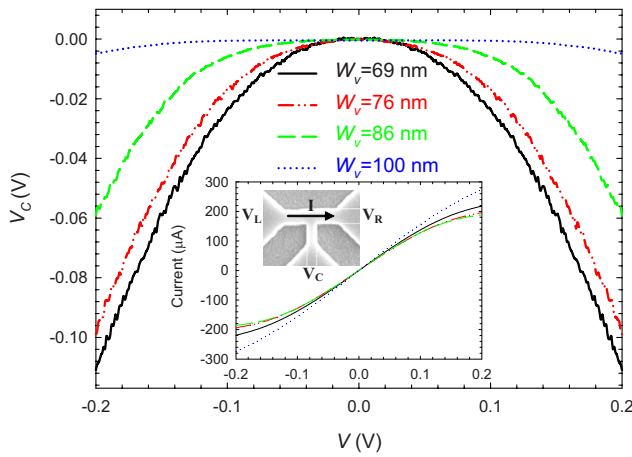


FIG. 3. (Color online) Values of the bottom potential V_C and current I (inset) measured in TBJ junctions with a width of the vertical branch W_V of 69, 76, 86, and 100 nm as a function of the push-pull bias V . $W_H = 500$ nm.

works essentially as a voltage probe.⁷ However, as shown by recent experiments, in the case of narrow branches close to be completely depleted, that is not the case, and the V_C response depends on W_V .¹⁰ As explained by means of the recently developed self-consistent surface charge model, for small W_V the surface charge in the sidewalls of the vertical branch and the carrier penetration inside it change with the bias, provoking that V_C is no longer a faithful reflection of the variations in potential in the center of the junction, which we will denote as V_{HC} . Therefore, the behavior of V_C can be considered as the result of two combined effects: a horizontal one (given by the variation of V_{HC} with the bias) associated with both ballistic transport and surface charges at the sidewalls of the horizontal branch and a vertical one (given by the variation of the potential profile along the vertical branch with the bias) associated with surface charges in the vertical branch.

To check that the previous behavior takes place also in wide TBJs, devices with $W_H = 500$ nm and different values of W_V (69, 76, 86, and 100 nm) have been fabricated and characterized. Results of measurements for the voltage V_C and the current I are presented in Fig. 3. As observed, the characteristic quadratic bell-shaped output voltage of TBJs is obtained, with higher curvature as W_V decreased, what indicates that the vertical branch is an active element of the device.¹⁰ I is practically the same in the four structures, small differences arising just because of unavoidable variations in the fabrication process. The resistance of the vertical branch has been also measured, providing values of 890, 120, 15, and 3.4 k Ω for W_V of 69, 76, 86, and 100 nm, respectively. The higher the resistance of the vertical branch, the more pronounced the curvature observed in the V_C - V curve.

IV. DISCUSSION: MONTE CARLO SIMULATIONS

By means of our MC simulator including the self-consistent surface charge model it is possible to explain the physical origin of the previous results. Simulation of TBJs with W_H higher than 500 nm requires unaffordable computation times. That is why, to explain the dependence of the

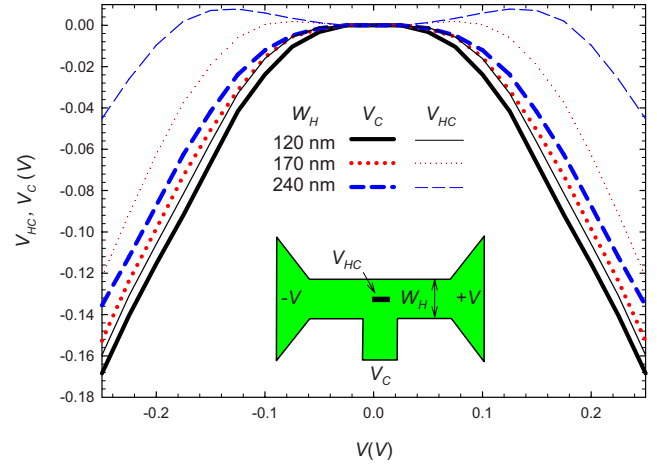


FIG. 4. (Color online) V_{HC} - V and V_C - V curves as obtained from MC simulations for TBJs with $W_H = 120, 170,$ and 240 nm. The width of the vertical branch W_V is 108 nm.

V_C - V curves on W_H , we will initially consider smaller values of W_H , from 120 to 240 nm, in TBJs with length of the horizontal branches of 250 nm and W_V of 108 nm (608 nm between left and right contact). As observed in Fig. 4, the values of V_C are more negative as W_H is decreased, according to the observed experimental trend (Fig. 1). The dependence on W_H of the potential at the center of the junction V_{HC} , also plotted in Fig. 4, is even more pronounced than that of V_C . To understand such behavior, Fig. 5(a) shows the profiles of carrier concentration and 5(b) the surface charge at the top boundary of the junction along the horizontal direction for $V = 0.25$ V. The narrower the horizontal branch, the lower the free carrier concentration due to the stronger depletion induced by the enhanced surface charge. For this reason the horizontal potential profile is different in each junction and also the value of V_{HC} . The asymmetry in the electron concentration profile, originated by the combined effect of ballistic transport and asymmetric surface charge, is enhanced by the reduction of W_H . Such an asymmetry provokes that most of the applied potential drops in the region near the anode (right contact), so that V_{HC} (and also V_C) takes negative values, higher for lower W_H . The dependence of V_{HC} on W_H is smoothed in the bottom potential V_C by the adaptation of surface charge in the vertical branch.¹⁰ Therefore, it is the role played by surface charge and the associated depletion what leads to the observed variations between structures with different W_H . The influence of surface charge on V_C is much stronger than that of ballistic transport in the case of small W_H , but decays sharply for wide TBJs, as indicated by Eq. (1).

It is also remarkable that in the wider TBJs, for the lowest applied voltages, V_{HC} gets slightly positive values before becoming negative. These positive values indicate that under such bias conditions the branch contacted to the cathode is more resistive than the anode one. As will be explained below, it is due to a velocity overshoot effect (more pronounced near the cathode) taking place for weak enough surface charge effects.

Using the same model we have simulated one of the fabricated TBJs reported in Figs. 1 and 3, the one with

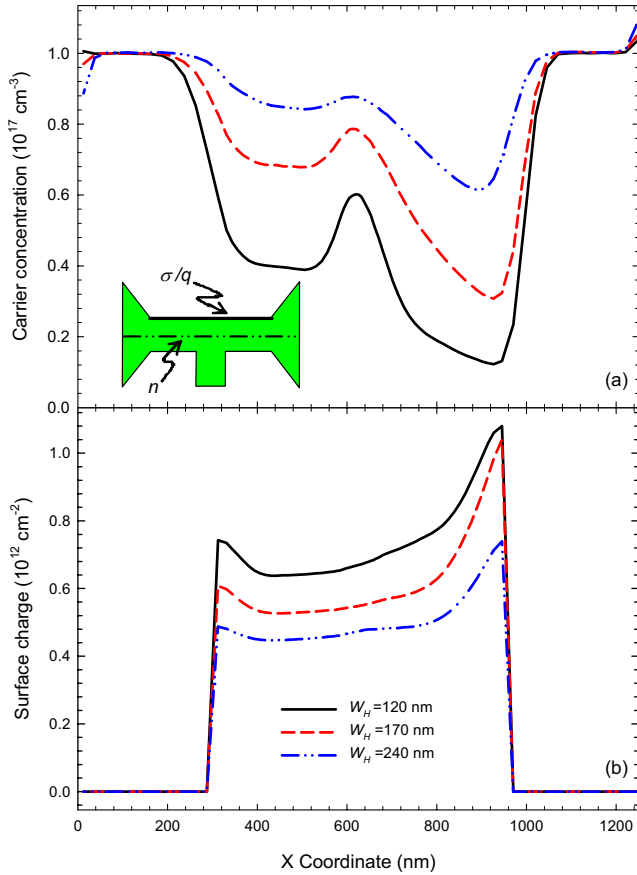


FIG. 5. (Color online) Profiles of (a) carrier concentration, n , along the horizontal direction (left axis) and (b) surface charge, σ/q , at the top boundary of the junction (right axis) in TBJs with $W_H = 120$, 170, and 240 nm for a push-pull bias $V = 0.25 \text{ V}$.

$W_H = 500 \text{ nm}$ and $W_V = 69 \text{ nm}$. The topology used in MC simulations, shown in Fig. 6(a), closely corresponds to the real one. As observed in Figs. 1 and 6(a), due to the large width of the horizontal branch, the size of the accesses is comparable to that of the active zone, so that the injection technique in simulations requires special attention, since part of the voltage drop may take place inside the accesses so that contacts are not strictly at equilibrium. To account for these effects, in this case we use an Ohmic injection scheme¹⁴ that imposes charge neutrality in the cells adjacent to the contacts, instead of the standard equilibrium injection rate typically considered in ballistic nanodevices.^{7,8} The results for both V_C and I , plotted in Fig. 6(b), exhibit an excellent agreement with the measurements, thus confirming the validity of our model.

The microscopic quantities provided by MC simulations allow understanding the origin of the differences between the response of TBJs with narrow and wide horizontal branches. To this end, we have simulated a TBJ with the same geometry of the previous one, except that $W_H = 120 \text{ nm}$. Several changes are observed from one junction to the other, mainly related to the influence of the surface charge and the degree of asymmetry between the left and right horizontal branches. First, the electron concentration for $W_H = 500 \text{ nm}$ is much more homogeneous than for the narrower TBJ. In the wide TBJ only a decrease in concentration of about 10% with

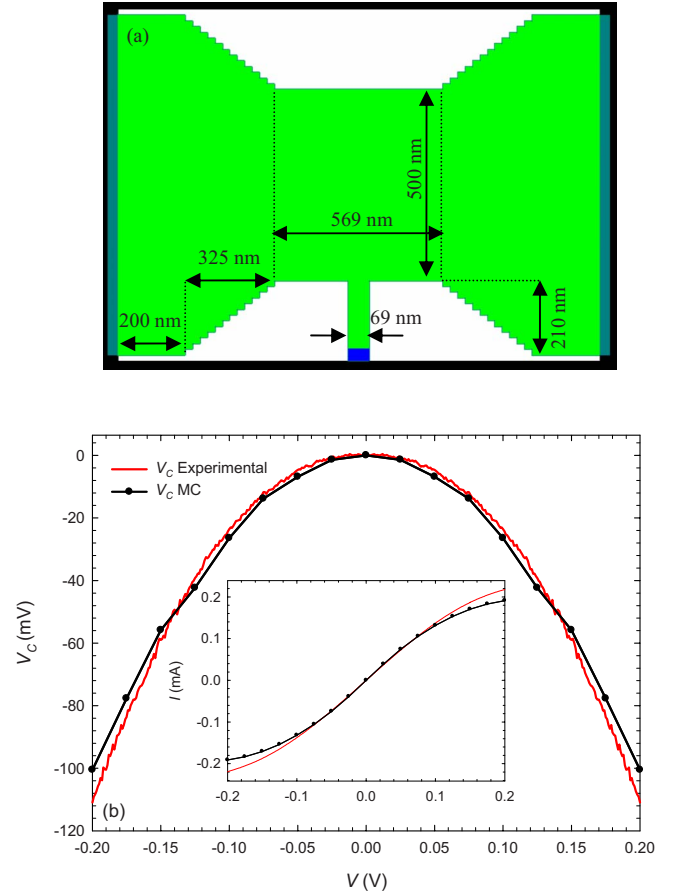


FIG. 6. (Color online) (a) Geometry of the MC simulation domain for the TBJ with $W_H = 500 \text{ nm}$. (b) Comparison of measured and simulated values of V_C vs push-pull bias V for the TBJ with $W_H = 500 \text{ nm}$. Inset: I - V curve obtained using a nonsimulated dimension $Z = 10^{-7} \text{ m}$.

respect to the background doping (similar in both horizontal branches) is observed, while in the narrow one, due to the stronger influence of surface charge, a strong depletion takes place, much more pronounced in the right branch. On the other hand, as explained before, due to the comparable transversal size of accesses and active region in the wide TBJ, a significant potential drop takes place in the accesses. We have checked that for a bias of 0.2 V nearly $\frac{1}{3}$ of the voltage drops outside the active region when $W_H = 500 \text{ nm}$, while for $W_H = 120 \text{ nm}$ the voltage drop in the accesses is almost negligible. The velocity profiles along the horizontal branch shown in Fig. 7 for both TBJs reflect the previous effects. The asymmetry is clearly stronger in the case of $W_H = 120 \text{ nm}$, velocity being much higher close to the anode due to the more intense electric field present in the right branch. The high values of velocity close to the contacts observed for $W_H = 500 \text{ nm}$ indicate the strong penetration of the electric field in the access regions. Indeed, even if the velocity seems to be higher in the narrow structure, when subtracting from the applied voltage the potential drop in the accesses, the maximum velocities reached in both junctions are similar. For example, comparing the curve for 0.2 V in the 500 nm TBJ with the one for $0.125 \text{ V} \approx (2/3) \times 0.2 \text{ V}$ in the 120 nm TBJ, both reach values about $3.5\text{--}4 \times 10^7 \text{ cm/s}$.

The efficiency of the rectifying behavior of both TBJs is

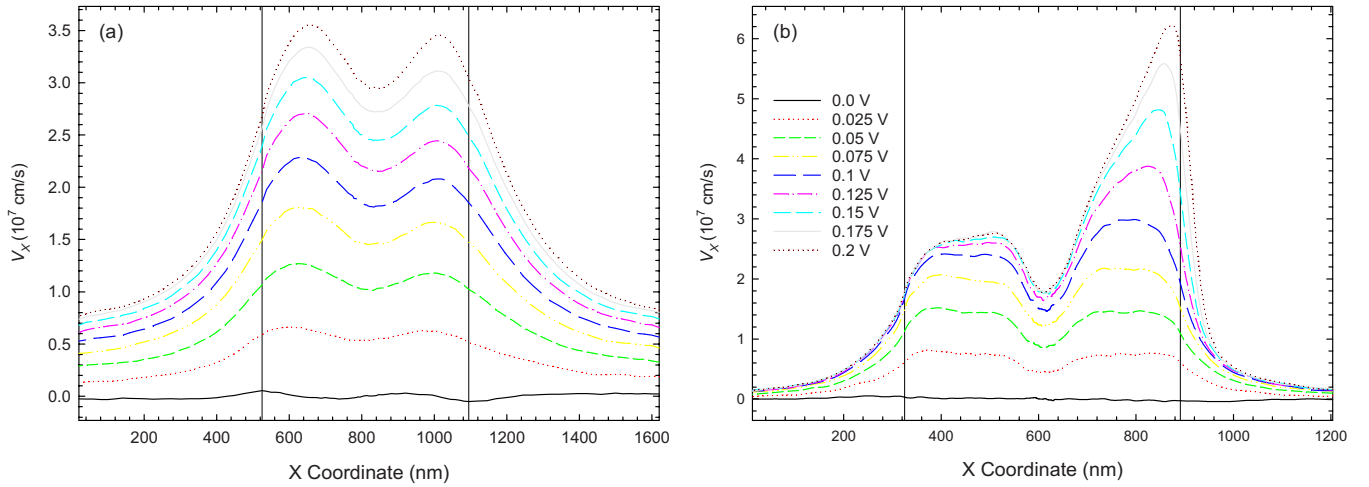


FIG. 7. (Color online) Profiles of longitudinal velocity along the horizontal branch for push-pull bias voltages between 0.0 and 0.2 V in TBJs with (a) $W_H = 500$ nm and (b) $W_H = 120$ nm. Vertical lines delimit the active region of each TBJ.

influenced by all these features. Figure 8 compares the simulations of V_C , V_{HC} , and the current through the horizontal branch I for both devices. We show the results obtained with the self-consistent surface charge model, in which the charge profiles are modified according to the bias conditions, and also with a “frozen” surface charge profile corresponding to

equilibrium conditions. The self-consistent results at $V = 0.1$ V provide $V_C = -44$ mV in the case of $W_H = 120$ nm, while $V_C = -26$ mV for $W_H = 500$ nm, which means nearly a factor of 2 in the efficiency. In both junctions, the V_C - V curve obtained with the frozen profile exhibits a smaller curvature (and thus a lower efficiency), what confirms the importance of considering the self-consistent surface charge model in calculations.

An important difference in the behavior of V_{HC} and I is observed between both junctions. In the case of $W_H = 500$ nm, the values of V_{HC} and I obtained with the frozen and the self-consistent surface charge profiles are practically the same, while for $W_H = 120$ nm they differ significantly. When the width of the horizontal branch is large, the influence of the surface charge at its boundaries is very small, and thus V_{HC} and I are nearly independent of the surface charge model. The increase in the difference of the values of V_C with respect to those of V_{HC} is essentially due to a vertical effect of electron penetration in the vertical branch as the applied voltage is increased. In the case of the narrow horizontal branch, the influence of the surface charge on the horizontal branches is much stronger, and V_{HC} and I differ a lot between both models. This means that, in contrast with the wide junction, the adaptation of the surface charge in the horizontal branch plays a role in the negative values of V_C , increasing the efficiency of the device.

The upper-bending trend observed in the shape of V_{HC} for the wider junction [Fig. 8(a)], and also when using the frozen equilibrium profile in the narrower one [Fig. 8(b)], is explained again as due to the strength of surface charge effects. In both cases the electric field is relatively uniform along the horizontal branches as a consequence of weak surface charge depletion (either because the large width of the branch or the use of the equilibrium profile). Under such conditions, as observed in Fig. 7(a), an overshoot effect takes place along the whole horizontal branches that is slightly more pronounced near the cathode (left contact in the figure). As a result, the branch close to the cathode has lower concentration and higher resistance as compared to the anode one, thus leading to the positive values of V_{HC} . This phenom-

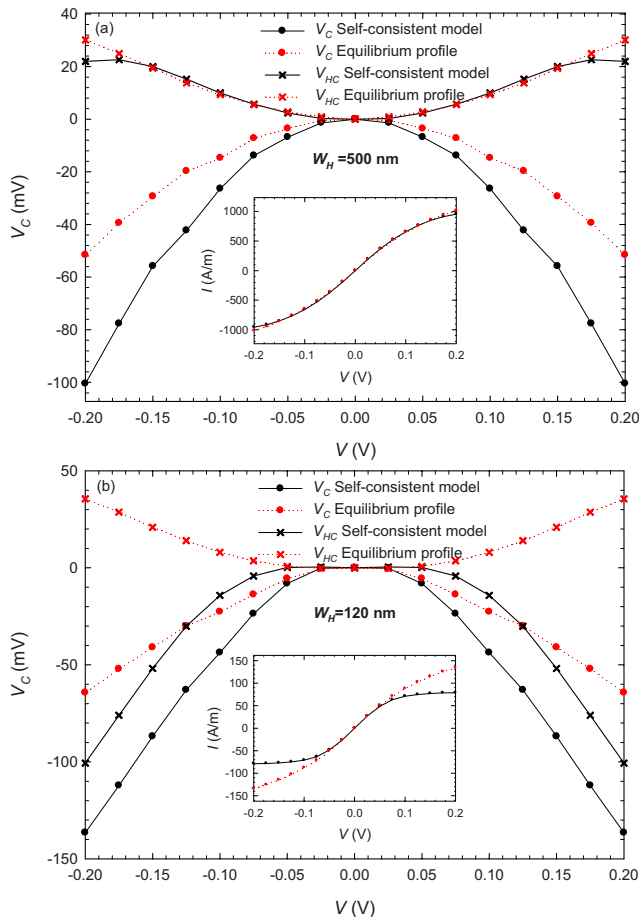


FIG. 8. (Color online) MC results for V_C - V and V_{HC} - V curves in TBJs with (a) $W_H = 500$ nm and (b) $W_H = 120$ nm simulated with the self-consistent surface charge model and also with the surface charge fixed to the equilibrium profile. Insets: current flowing through the horizontal branch.

enon was already observed in previous works,⁸ when very low values of (constant) surface charge were used in the modeling of TBJs. In contrast, when the branch is narrow and the effect of the surface charge is notable, like in Fig. 8(b) when using the self-consistent model, electrons are mainly accelerated in the region near the anode, where the electric field is significantly higher, as observed in Fig. 7(b). In this case the resistance of the anode zone is manifestly the largest one in the device, providing the negative values of V_{HC} .

V. CONCLUSIONS

$\text{In}_{0.52}\text{Al}_{0.48}\text{As}/\text{In}_{0.75}\text{Ga}_{0.25}\text{As}$ TBJs with different widths of the horizontal and vertical branches have been fabricated and characterized in dc conditions. Measurements show that the typical parabolic behavior of the output voltage at the bottom of the vertical branch persists when the width of the horizontal branches is enlarged, even for very wide junctions (horizontal branch much wider than the electron mean free path), but the efficiency of the rectifying response is reduced. An increase in the width of the vertical branch also leads to a reduction in the efficiency at the output.

By means of an ensemble MC simulator self-consistently coupled with a 2D Poisson solver, and making use of a self-consistent model of surface charge, the origin of the behavior observed in measurements has been explained. The lower depletion and longitudinal asymmetry induced by the surface charge at the boundaries of the horizontal branches as these become wider has been found at the origin of the reduction in the efficiency of the rectifying response. In the case of increased width of the vertical branch, the lower efficiency is due to the less significant influence of surface charges at the boundaries of the vertical branches, which change with the geometry and the applied bias.

From the point of view of applications, the fact that by widening the horizontal branches the parabolic response persists can be very useful, even if the efficiency is lower, since it allows reducing the input impedance of the devices, thus making easier their matching to 50 Ω systems and avoiding

an strong degradation due to extrinsic capacitances. A trade-off between efficiency and low-enough impedance should determine the width of horizontal branches in TBJs for each specific application.

ACKNOWLEDGMENTS

This work has been partially supported by the Dirección General de Investigación (MEC, Spain), by FEDER through Project No. TEC2007-61259/MIC, by the Consejería de Educación of the Junta de Castilla y León (Spain) through Project No. SA019A08, and by the French Research Ministry through Project No. ACI JC9015.

- ¹A. M. Song, A. Lorke, A. Kriele, and J. P. Kotthaus, *Phys. Rev. Lett.* **80**, 3831 (1998).
- ²I. Shorubalko, H. Q. Xu, I. Maximov, P. Omling, L. Samuelson, and W. Seifert, *Appl. Phys. Lett.* **79**, 1384 (2001).
- ³L. Worschech, D. Hartmann, S. Reitzenstein, and A. Forchel, *J. Phys.: Condens. Matter* **17**, R775 (2005).
- ⁴J. Sun, D. Wallin, I. Maximov, and H. Q. Xu, *IEEE Electron Device Lett.* **29**, 540 (2008).
- ⁵S. Bollaert, A. Cappy, Y. Roelens, J. S. Galloo, C. Gardès, Z. Teukam, X. Wallart, J. Mateos, T. Gonzalez, B. G. Vasallo, B. Hackens, L. Berdnar, and I. Huynen, *Thin Solid Films* **515**, 4321 (2007).
- ⁶H. Irie, Q. Diduck, M. Margala, R. Sobolewski, and M. J. Feldman, *Appl. Phys. Lett.* **93**, 053502 (2008).
- ⁷J. Mateos, B. G. Vasallo, D. Pardo, T. González, J. S. Galloo, Y. Roelens, S. Bollaert, and A. Cappy, *Nanotechnology* **14**, 117 (2003).
- ⁸J. Mateos, B. G. Vasallo, D. Pardo, T. González, J. S. Galloo, S. Bollaert, Y. Roelens, and A. Cappy, *IEEE Trans. Electron Devices* **50**, 1897 (2003).
- ⁹J. Mateos, B. G. Vasallo, D. Pardo, T. González, E. Pichonat, J. S. Galloo, S. Bollaert, Y. Roelens, and A. Cappy, *IEEE Electron Device Lett.* **25**, 235 (2004).
- ¹⁰I. Iñiguez-de-la-Torre, J. Mateos, T. González, D. Pardo, J. S. Galloo, S. Bollaert, Y. Roelens, and A. Cappy, *Semicond. Sci. Technol.* **22**, 663 (2007).
- ¹¹H. Q. Xu, *Appl. Phys. Lett.* **78**, 2064 (2001).
- ¹²D. Wallin, I. Shorubalko, H. Q. Xu, and A. Cappy, *Appl. Phys. Lett.* **89**, 092124 (2006).
- ¹³J. S. Galloo, E. Pichonat, Y. Roelens, S. Bollaert, X. Wallart, A. Cappy, J. Mateos, and T. González, Proceedings of the 2004 International Conference on Indium Phosphide and Related Materials IPRM, IEEE Catalog 04CH37589, 2004, 378; http://ieeexplore.ieee.org/xpls/abs_all.jsp?isnumber=30998&arnumber=1442734&count=202&index=101.
- ¹⁴T. González and D. Pardo, *Solid-State Electron.* **39**, 555 (1996).